Self-Organized Vertical Superlattices in Epitaxial GaInAsSb

C.A. Wand, C.J. Vineis and D.R. Calawa

NOTICE

\

Self-Organized Vertical Superlattices in Epitaxial GaInAsSb*

C.A. Wang, C.J. Vineis[†], and D.R. Calawa

Lincoln Laboratory, Massachusetts Institute of Technology, Lexington, MA 02420-9108

[†]now at AmberWave Systems Corporation, Salem, NH 03079

ABSTRACT

Self-organized superlattices are observed in GaInAsSb epilayers grown nominally lattice matched to vicinal GaSb substrates. The natural superlattice (NSL) is detected at the onset of growth; is continuous over the lateral extent of over several microns; and persists vertically throughout several microns of the epilayer. Furthermore, the NSL is inclined by an additional 4° with respect to the vicinal (001) GaSb substrate. The tilted NSL intersects the surface of the epilayer, and the NSL period is geometrically correlated with surface undulations. While the principle driving force for this type of phase separation arises from solution thermodyamics, the mechanism for the self-organized microstructure is related to local strains associated with surface undulations. By using a substrate with surface undulations, the tilted NSL can be induced in layers with alloy compositions that normally do not exhibit this self-organized microstructure under typical growth conditions. These results underscore the complex interactions between compositional modulations and morphological perturbations.

Phase separation in multi-component compound semiconductors has been widely reported [1]. Of particular interest are materials systems that spontaneously self-organize with a significant degree of regularity, since this periodicity can impact the electronic band structure and consequently, materials properties and device performance. The length scale of these ordered phases ranges from the atomic scale, e.g. CuPt ordering as observed in GaInP [2], GaAsP [3], GaAsSb, [4], and InAsSb [5], to microscopic dimensions on the order of ~50 nm, e.g. composition modulation. Composition modulation can persist either parallel (lateral) to the growth direction, or perpendicular (vertical) to the growth direction. Lateral composition modulation (LCM) has been reported in strained alloy systems such as bulk AlInAs and GaInP epilayers [6-8], as well as in short period superlattices such as GaP/InP, AlAs/InAs, GaAs/InAs, and InAs/GaSb [9-11].

Vertical composition modulation (VCM) and self-organized natural superlattices (NSLs) in alloy layers that are homogenously grown have also been observed, but these studies are less frequently reported and the mechanism for the self-organization is less understood. NSLs have been reported in ZnSeTe grown on vicinal GaAs substrates [12] and SiGe grown on (001) Si [13]. The NSL period was 2 to 3 nm for both of these materials systems, and a model based on step-flow growth and local strain fields that are modulated during growth were developed to explain the phenomena [13]. In addition, InAsSb and GaAsSb [5,14] were reported to spontaneously form a periodic structure that consisted of platelets of alternating composition and periodicity on the order of 20 to 50 nm. Both InAsSb and GaAsSb exhibit miscibility gaps [15], and this larger scale modulation was attributed to the tendency for these alloys to phase separate. It was speculated that islands of the different phases develop at the growth surface and then subsequently laterally overgrow each other. While atomic ordering and VCM were

2

simultaneously observed in InAsSb and GaAsSb [5], VCM without ordering was reported for GaInP [16]. The periodicity of the VCM was 10 to 12 nm. More recently, spontaneous superlattice formation was observed for GaInAsSb [17], AlGaInN [18] and AlGaInAsSb [19]. The NSLs have modulation period ranging 10 to 30 nm.

This work reports spontaneous formation of self-organized NSLs in GaInAsSb alloys grown nominally lattice matched to vicinal GaSb substrates. The NSL is inclined 4° with respect to the substrate miscut angle. Furthermore, the NSL period is geometrically matched with the periodicity of undulations on the epilayer surface. This correlation clearly demonstrates the intimate coupling between composition modulation and morphological perturbations [20-23].

GaInAsSb epitaxial layers were grown nominally lattice matched to (001) GaSb substrates with miscut angles of 2 or 6° toward (1-11)B or (101) by OMVPE as previously described [24-25]. The growth temperature was either 525 or 575 °C. Trimethylindium, triethylgallium, tertiarybutylarsine, and trimethylantimony were used as organometallic precursors. Growth was initiated by simultaneously flowing the four precursors into the OMVPE reactor. The growth rate was ~5 µm/hr, and the layers were 1 to 4 µm in thickness. Two different alloy compositions were grown: $Ga_{0.89}In_{0.11}As_{0.09}Sb_{0.91}$ and $Ga_{0.8}In_{0.2}As_{0.17}Sb_{0.83}$, which have 300 K photoluminescence (PL) peak energy at 0.6 eV and 0.5-eV, respectively. The GaInAsSb alloy composition was determined from the peak energy in 300 K PL spectra and lattice mismatch, as previously described [24]. The microstructure of GaInAsSb was studied by examining <110> cross-sections in TEM operated at 200 kV. The NSL was imaged using g = <222> or <111> 2-beam conditions, in either bright- or dark-field conditions. Characterization also included photoluminescence (PL) at 300 and 4K and atomic force microscopy (AFM) operating in tapping mode.

Figures 1a and 1b shows bright-field (BF) <110> cross-section TEM images of 0.6-eV $Ga_{0.89}In_{0.11}As_{0.09}Sb_{0.91}$ and 0.5-eV $Ga_{0.8}In_{0.2}As_{0.17}Sb_{0.83}$, respectively. The layers were grown at 525 °C on (001) GaSb substrates miscut 6° toward (1-11)B. Minimal TEM diffraction contrast is observed for 0.6-eV GaInAsSb, while significant spinodal-like contrast [1] is observed for 0.5-eV GaInAsSb. This contrast results from the strain that is associated with phase separation into GaAs- and InSb-rich regions [24,25] and is consistent with the 0.5-eV GaInAsSb alloy being further in the miscibility gap [15]. The 4 K PL FWHM of these samples was 4.3 and 9.5 meV, respectively for Fig. 1a and 1b, respectively. The value for the sample in Fig. 1b is considerably small despite the inhomogeneity of the microstructure.

In addition to the spinodal-like contrast observed in 0.5-eV GaInAsSb, Fig. 2 shows the presence of a self-organized NSL in <110> TEM cross-sections. The image shown in Fig. 2a is a [110] cross-section, which is parallel with step-flow direction [25], and was obtained using a dark-field (DF) <222> 2-beam condition. The NSL has a 10° tilt with respect to the surface normal, which is an additional 4° compared to the 6° miscut angle. The NSL is observed at the onset of growth; is laterally continuous throughout the epilayer; and has a periodicity of 20 nm throughout the 2-μm-thick epilayer. Figure 2b is the orthogonal [-110] cross-section (perpendicular to step-flow) and shows that in this direction, the NSL is parallel to the growth surface. Figure 2c schematically shows the geometry of the microstructure. It is interesting to also note that the NSL could also be imaged in field-emission scanning electron microscopy (images not shown here) and the results are consistent with TEM. No tilted superlattice was detected in the 0.6-eV GaInAsSb.

The AFM image of 0.6-eV GaInAsSb, Fig. 3a, shows that the surface morphology is relatively smooth and flat. Conversely, the AFM image of 0.5-eV GaInAsSb, Fig. 3b, exhibits a

periodic surface undulation that is aligned along the step edges of the vicinal substrate. The tilted NSL will intersect the surface of the epilayer, and it was found that the periodicity of these surface undulations is directly correlated with the period of the tilted NSL. The tilted NSL has a period of 20 nm and a tilt angle of 10°. Simple geometry indicates that its intersection with the surface corresponds to a length of 115 nm. The surface undulation of the AFM image shown in Fig. 3b has a lateral period of about 111 nm. Thus, the period of the tilted NSL and the period of the surface undulations are the same. Table I shows several examples of this correlation. Note that additional tilt angle with respect to the substrate miscut angle is about 4°. It was also found that all GaInAsSb epilayers having a tilted superlattice also exhibit periodic surface undulations, and that the amplitude of the surface undulation increases with the strength of the tilted NSL [26]. Both of these features are concurrently observed with spinodal-like contrast, and thus, appear to be a consequence of phase separation.

These results suggest that the tilted NSL and surface undulations are coupled, and furthermore depend on the thermodynamic driving force for phase separation. To study this hypothesis, a test structure was specially grown. The layer structure, Fig. 4a, consists of different alloy compositions of GaInAsSb, layers #1, #3, and #5, separated by 2 nm GaSb, layers #2 and #4. Layers #1 and #5 are 0.6-eV GaInAsSb, while layer #3 is 0.5-eV GaInAsSb. Based on the results shown in Figs. 1 and 2, spinodal-like contrast and a tilted NSL are anticipated in layer #3, but not in layers #1 and #5. Figure 4b of the cross-section <222> 2-beam TEM image indicates no tilted NSL in layer #1 and a tilted NSL in layer #3, as expected. Figure 4c shows that the tilted NSL present in layer #3 induces a tilted NSL in layer #5, even though the NSL was not present in layer #1 and layers #1 and 5 were grown under the same temperature and flow conditions. Although the contrast modulation associated with the NSL in layer #5 is weaker, the

periodicity is the same layers #3 and #5. These images clearly illustrate the coupling of compositional and morphological perturbations [20-23]. The composition associated with layer #5 does not inherently phase separate to form a tilted NSL, but it did so in this special case because surface undulations present from layer #3 created surface stresses that drive lateral surface segregation. The lateral period of the surface undulation is about 100 nm, and correlates with the tilted NSL, which had a period of 17.2 nm and a tilt angle of 9.7°, yielding a lateral period of [17.2 nm / sin (9.7°)] = 102 nm.

A qualitative model for the initial formation of the tilted NSL and its propagation throughout the epilayers is proposed. Due to the thermodynamic driving force of the miscibility gap, adatoms segregate to form a lateral composition modulation, with one phase slightly enriched in InSb and another slightly enriched in GaAs. Once such lateral composition modulation forms, the surface is strained due to the lattice-mismatch between the two GaInAsSb phases enriched in GaAs and InSb. As Glas has recently shown theoretically [23], a surface with such a lateral composition modulation can effectively relieve its strain if the larger lattice constant phase (InSb-rich phase) forms peaks, while the smaller lattice constant phase (GaAs-rich phase) forms valleys. Therefore, the surface forms a series of peaks and valleys, creating surface undulations, as are observed in the AFM images in Fig. 3b. Once such undulations form, all subsequent epitaxial deposition is biased to minimize surface stresses so that surface peaks preferentially incorporate InSb-enriched GaInAsSb, while the surface valleys preferentially incorporate GaAs-enriched GaInAsSb. Thus, this strain locking causes the NSL to continually propagate throughout epilayer growth. Therefore, the composition modulation associated with the tilted NSL is directly coupled to the surface undulations, and shows that surface strain or roughness can promote phase separation. Such strain-locking mechanisms due to surface stress are known

to play important roles in other epitaxial phenomena such as the vertical registry of multiple layers of quantum dots.

The mechanism for the additional tilt of the NSL with respect to surface steps can be explained in part by mechanism suggested by Venezuela et al. [13]. The model is based on alloy decomposition at step bunches, which are compressively and tensilely strained at the base and top of the bunch, respectively. NSL formation with a period on the order of the step-bunch height of a few nm and with an additional tilt angle with respect to the substrate miscut angle was predicted for alloys grown on surfaces with modulated strain fields. However, since the NSL periods observed in this study are on the order of 20 nm, that model cannot fully explain the larger NSL periods observed here. Therefore, it is proposed that surface undulations can play a similar role to step bunches in the Venezuela model. Rather than ejection and capture of single steps from step bunches, in this case the additional tilt is caused by ejection and capture of single steps from surface peak or valley regions. The lateral period of the undulations is typically 100-200 nm. Each peak or valley region is therefore 50-100 nm, and thus comprises on average 17-34 individual steps (for a 6° miscut) or 6-11 steps (for a 2° miscut). As epitaxial growth proceeds, if an individual step is ejected by a valley and captured by an adjacent peak, that step would switch its incorporation preference from GaAs-enrichment to InSb-enrichment. Similarly, that step would eventually be ejected from the peak and captured by the adjacent valley, switching its preference back to GaAs-enrichment. The magnitude of the additional tilt with respect to the substrate miscut angle is dependent on the relative lateral velocities of the surface undulations and the individual steps that comprise those undulations.

In conclusion, self-organized NSL are observed in GaInAsSb epilayers. The NSL exhibits a 4° tilt with respect to the miscut angle of the GaSb substrate, and the NSL period is directly

correlated with periodic undulations on the epilayer surface. The undulations form to relieve the local strain associated with composition modulation of the tilted NSL and demonstrates the coupling between composition modulation and morphological perturbations. A qualitative model for the propagation and robustness of the tilted NSL is discussed.

REFERENCES

1. A. Zunger and S. Mahajan, Handbook of Semiconductors, edited by T.S. Moss (Elsevier Science, Amsterdam, 1994), Vol. 3, p. 1399.

2. T. Suzuki, A. Gomyo, and S. Iijima, J. Cryst. Growth 93, 396 (1988).

3. G.S. Chen, D.H. Jaw, and G.B. Stringfellow, Appl. Phys. Lett. 57, 2475 (1990).

4. H.R. Jen, M.J. Jou, Y.T. Cherng, and G.B. Stringfellow, J. Cryst. Growth 85, 175 (1987).

5. A.G. Norman, T.-Y. Seong, I.T. Ferguson, G.R. Booker, and B.A. Joyce, Semicond. Sci. Technol. 8, S9 (1993).

6. S.W. Jun, T.-Y. Seong, J.H. Lee, and B. Lee, Appl. Phys. Lett. 68, 3443 (1996).

7. B. Shin, A. Lin, K. Lappo, R.S. Goldman, M.C. Hanna, S. Francoeur, A.G. Norman, and A. Mascarenhas, Appl. Phys. Lett. 80, 3292 (2002).

8. X. Wallart, C. Priester, D. Deresmes, and F. Mollot, Appl. Phys. Lett. 77, 253 (2000).

9. K.C. Hsieh, J.N. Baillargeon, and K.Y. Cheng, Appl. Phys. Lett. 57, 2244 (1990).

10. C. Dorin and J. Mirecki Millunchick, J. Appl. Phys. 91, 237 (2002).

11. D.W. Stokes, R.L. Forrest, J.H. Li, S.C. Moss, B.Z. Nosho, B.R. Bennett, L.J. Whitman, and M. Goldenberg, J. Appl. Phys. 93, 311 (2003).

12. S.P. Ahrenkiel, S.H. Xin, P.M. Reimer, J.J. Berry, H. Luo, S. Short, M. Bode, M. Al-Jassim, J.R. Buschert, and J.K. Furdyna, Phys. Rev. Lett. 75, 1586 (1995).

13. P. Venezuela, J. Tersoff, J.A. Floro, E. Chason, D.M. Follstaedt, F. Liu, M.G. Lagally, Nature 397, 678 (1999).

14. I.T. Ferguson, A.G. Norman, B.A. Joyce, T.-Y. Seong, G.R. Booker, R.H. Thomas, C.C. Phillips, and R.A. Stradling, Appl. Phys. Lett. 59, 3324 (1991).

15. G.B. Stringfellow, J. Cryst. Growth 58, 194 (1982).

16. D.M. Follstaedt, R.P. Schneider, Jr., and E.D. Jones, J. Appl. Phys. 77, 3077 (1995).

17. Y.-C. Chen, V. Bucklen, K. Rajan, C.A. Wang, G.W. Charache, G. Nichols, M. Freeman, and P. Sander, Mat. Res. Soc. Symp. Proc. Vol. 583, 367 (2000).

18. N.A. El-Masry, M.K. Behbehani, S.F. LeBoeuf, M.E. Aumer, J.C. Roberts, and S.M. Bedair, Appl. Phys. Lett. 79, 1616 (2001).

19. D.H. Jaw, J.R. Chang, and Y.K. Su, Appl. Phys. Lett. 82, 3883 (2003).

20. J. Tersoff, Phys. Rev. B56, R4394 (1997).

21. F. Glas, J. Appl. Phys. 62, 3201 (1987).

22. F. Glas, Appl. Surf. Sci. 123/124, 298 (1998).

23. F. Glas, Phys. Rev. B 62, 7393 (2000).

24. C.A. Wang, H.K. Choi, S.L. Ransom, G.W. Charache, L.R. Danielson, and D.M. DePoy, Appl. Phys. Lett. 75, 1305 (1999).

25. C.A. Wang, Appl. Phys. Lett. 76, 2077 (2000).

26. C.J. Vineis, Ph.D. Thesis, Massachusetts Institute of Technology, 2001.

TABLE

Table I. Correlation of Tilted Superlattice and Surface Undulations				
Miscut Angle	**NSL Period**	**NSL Tilt Angle**	**NSL Lateral Period**	**AFM Period**
6° [1-11]B	20 nm	10°	115 nm	111 nm
2° [1-11]B	14.6 nm	5.8°	144 nm	143 nm
2° [101]	13.8 nm	6.0°	132 nm	160 nm
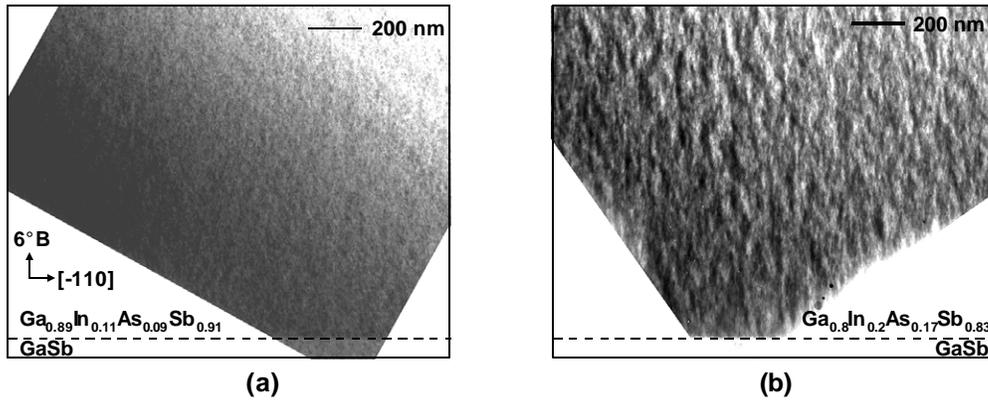
Figure 1. Bright field <110> cross-section TEM images using g = <220> 2-beam diffraction of GaInAsSb grown at 525 °C on substrates oriented (001) 6° toward (1-11)B: (a) $Ga_{0.89}In_{0.11}As_{0.09}Sb_{0.91}$ and (b) $Ga_{0.8}In_{0.2}As_{0.17}Sb_{0.83}$. The images are oriented so that the growth direction is straight up. The sample in (b) has a composition that was further into the miscibility gap than that in (a), and exhibits stronger spinodal-like contrast.
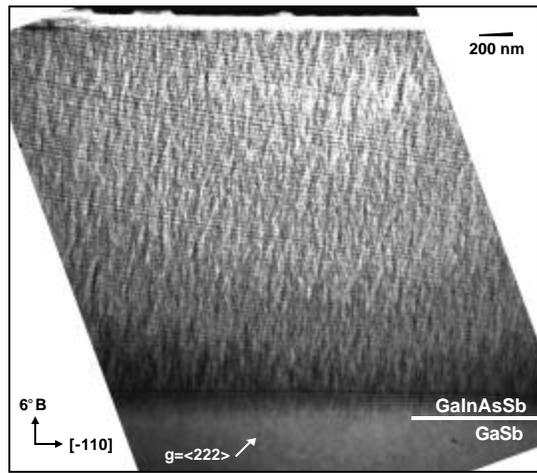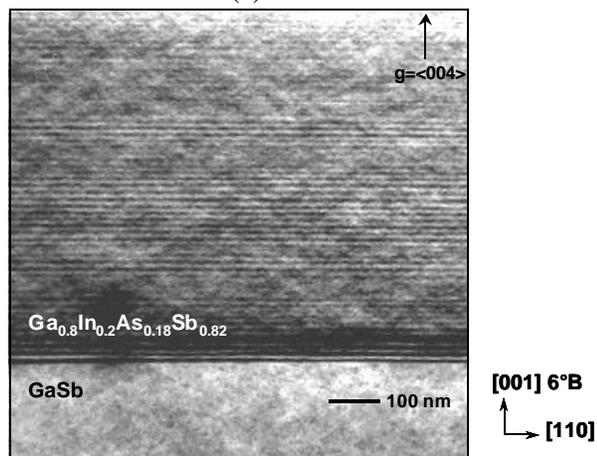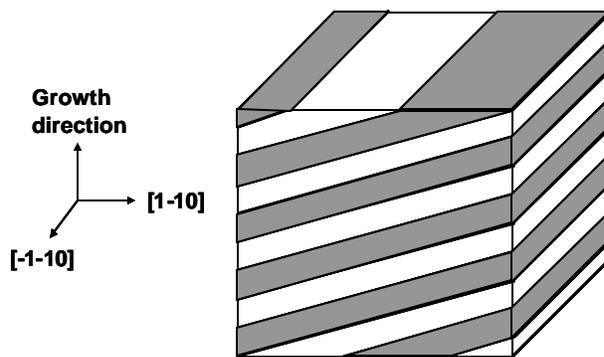
Figure 2. TEM images and schematic microstructure of $Ga_{0.8}In_{0.2}As_{0.17}Sb_{0.83}$: (a) [110] cross-section using g = <222> 2-beam conditions; (b) [-110] cross-section using g = <004> 2-beam conditions; (c) three-dimensional schematic of tilted NSL microstructure.

(a)

(b)
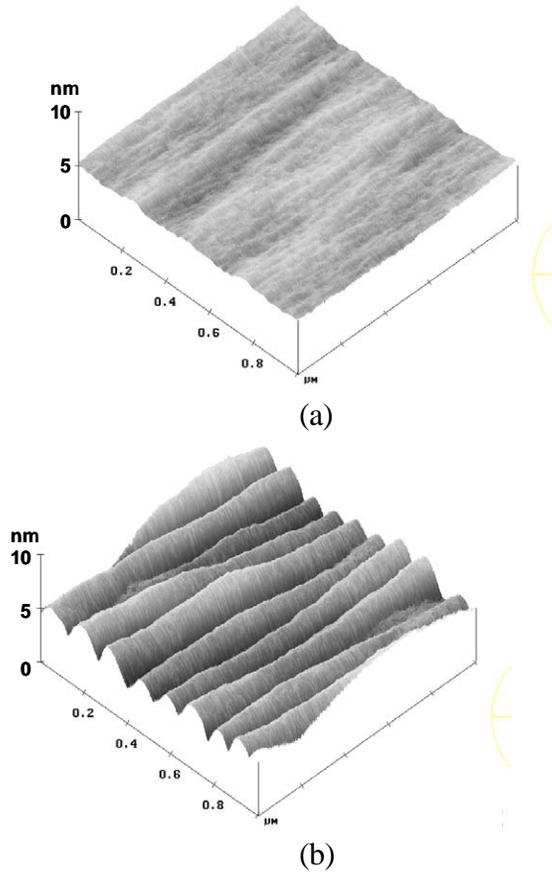
Figure 3. AFM images of the surface undulations of GaInAsSb samples grown on various GaSb substrate miscut orientations: (a) 0.6-eV GaInAsSb with no tilted NSL on (001) 6° toward [1-11]B and (b) 0.5-eV GaInAsSb with a tilted NSL on (001) 6° toward [1-11]B.

(a)

(b)

(c)

Figure 4. (a) Schematic test structure cross section; (b) <222> 2-beam diffraction of layers #1 - #3; (c) <222> 2-beam diffraction of layers #3 - 5.